ACS Chemical Neuroscience

Research Article

pubs.acs.org/chemneuro

Design, Synthesis, and Evaluation of Multitarget-Directed Selenium-Containing Clioquinol Derivatives for the Treatment of Alzheimer's Disease

Zhiren Wang, Yali Wang, Wenrui Li, Fei Mao, Yang Sun, Ling Huang,* and Xingshu Li*

Institute of Drug Synthesis and Pharmaceutical Processing, School of Pharmaceutical Sciences, Sun Yat-sen University, Guangzhou 510006, China

Supporting Information

ABSTRACT: A series of selenium-containing clioquinol derivatives were designed, synthesized, and evaluated as multifunctional anti-Alzheimer's disease (AD) agents. In vitro examination showed that several target compounds exhibited activities such as inhibition of metal-induced Aβ aggregation, antioxidative properties, hydrogen peroxide scavenging, and the prevention of copper redox cycling. A parallel artificial membrane permeation assay indicated that selenium-containing clioquinol derivatives possessed significant blood-brain barrier (BBB) permeability. Compound **8a**, with a propynylselanyl group linked to the oxine, demonstrated higher hydrogen peroxide scavenging and intracellular antioxidant activity than clioquinol. Furthermore, **8a** exhibited significant inhibition of Cu(II)-induced Aβ_{1-42} aggregation and was capable of disassembling the preformed Cu(II)-induced Aβ aggregates. Therefore, **8a** is an excellent multifunctional promising compound for development of novel drugs for AD.

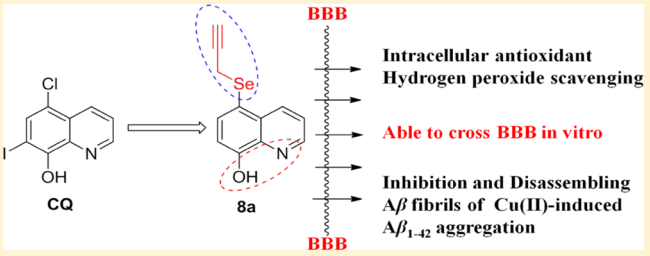

KEYWORDS: *Alzheimer's disease, selenium-containing clioquinol derivatives, antioxidative properties, inhibition of metal-induced Aβ aggregation*

Alzheimer's disease (AD), a multifaceted, progressive neurodegenerative disorder characterized by progressive cognitive decline and memory loss, results in serious personal and economic costs due to its high prevalence, mortality, and the elusiveness of efficacious drugs.[1] At present, several factors, including low levels of acetylcholine, β-amyloid (Aβ) deposits, τ-protein aggregation, oxidative stress, inflammation, and dyshomeostasis of biometals, play crucial roles in the pathogenesis of AD.[2]

Biometals, such as Cu(II), Zn(II), and Fe(II, III), are closely related to several critical aspects of AD, which suggests that the modulation of these biometals in the brain may be a potential therapeutic strategy.[3−6] Recently, biometal chelators (Figure 1) such as desferrioxamine (DFO), ethylenediaminetetraacetate (EDTA), clioquinol (CQ), tacrine-8-hydroxyquinoline hybrids, and M30 have been investigated.[7,8]

As is well-known, oxidation-induced apoptosis and tau-induced neurodegeneration could lead to the generation of Aβ, and oxidative stress was indicated in the onset and progression of AD pathology.[9] Protection of neurons from oxidative stress by the detoxification of reactive oxygen species (ROS) is crucial for AD patients as the efficacy of the endogenous antioxidant protection system declines sharply with age. It is thought that these mechanisms coexist and affect each other at multiple levels.[10] In this respect, multifunctional agents that simultaneously inhibit two or several targets (such as cholinesterase, Aβ aggregation), antioxidation and chelate redox-active metals

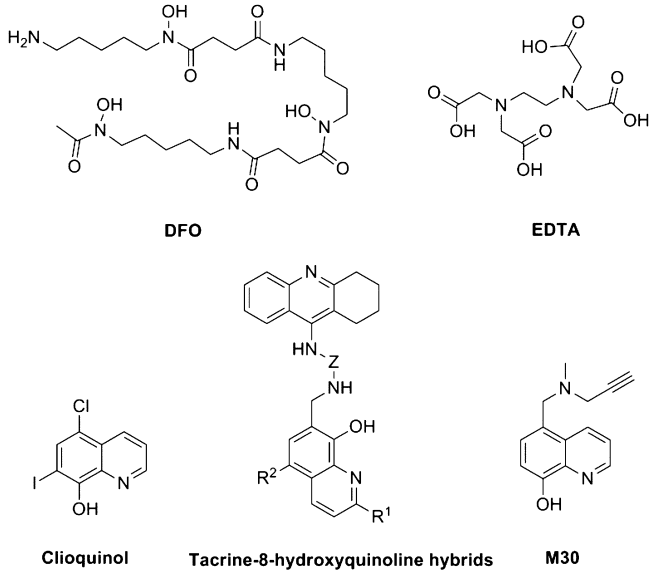

Figure 1. Chemical structures of metal-chelating agents.

Received: May 30, 2014
Revised: July 28, 2014
Published: August 14, 2014

Scheme 1. Synthesis of 2, 3, 4, 5, 6, 7a−7i, and 8a−8i[a]

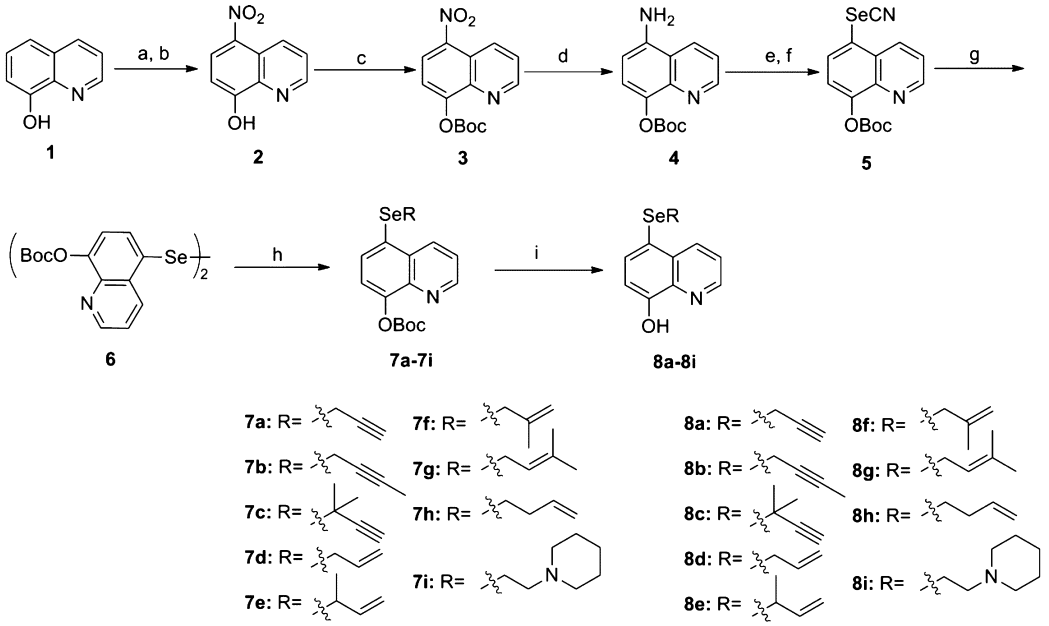

[a]Reagents and conditions: (a) H_2O, $NaNO_2$, H_2SO_4, 15−18 °C; (b) H_2O, HNO_3, rt; (c) CH_2Cl_2/hexane = 1:1, $(Boc)_2O$, DIPEA, DMAP, rt, 16 h; (d) EtOAc, $SnCl_2{\cdot}2H_2O$, rt, 3 h; (e) 10% HCl, H_2O, $NaNO_2$, −3 °C; (f) NaOAc, KSeCN; (g) CH_3OH, KOH; (h) EtOH, H_2O, $NaBH_4$, alkyl halide; (i) CH_2Cl_2, piperidine.

have been developed as potential agents for the treatment of AD.

Mineral selenium, an essential nutrient, demonstrated fundamental significance in human biology and fulfilled a multitude of indispensable health effects.[11−13] The redox cycle of selenium(II)/(IV) is thought to be the most important mechanism linked to biological systems by the reduction of ROS,[14,15] which are evolved in the oxidative damage of neurodegenerative diseases, such as AD and Parkinson's disease.[11,16−18] Over the past decades, selenium-containing compounds have attracted considerable interest in biology and chemistry due to their highly promising function.[12,19−23]

The propargyl moiety is known to be responsible for providing neuroprotective,[24−26] mitochondria-protecting,[27−29] antioxidant and scavenge peroxynitrite properties.[30] In recent studies, a series of propargyl moiety containing lead compounds, including (*S*)-rasagiline, TVP-1022, M30, and ladostigil, have been proven to exhibit neuroprotective activty in cell cultures and animal models of neurodegenerative diseases.[31−34] Moreover, the hydrophobicity of propargyl moiety is beneficial to enhance the BBB penetration ability.

Previously, we designed and synthesized a series of selenium-containing multifunctional anti-AD agents based on the fusion of donepezil and ebselen, and they exhibited GPx-like activity and inhibited the activity of AChE.[35,36] Herein, we describe the design, synthesis, and evaluation of a series of selenium-containing CQ derivatives as multifunctional anti-AD agents that exhibit inhibition of metal-induced Aβ aggregation, antioxidative properties, and hydrogen peroxide scavenging activity.

CHEMISTRY

Scheme 1 depicts the synthetic route of compounds **2**−**8**. The synthesis of the intermediates **2** and **3** was conducted as previously described.[37−39] The reduction of **3** with $SnCl_2{\cdot}2H_2O$ afforded amine **4**. Diazotization of **4** with $HCl/NaNO_2$ followed by reaction with KSeCN provided the selenocyanate **5**. Intermediate **5** was treated with KOH in CH_3OH to give the diselenide **6**, which was reacted with sodium borohydride and alkyl halides to afford the corresponding 5-alkylselenenyl-quinolin derivatives **7**. Finally, the deprotection of the Boc group in the presence of piperidine yielded the target compounds **8**.

RESULTS AND DISCUSSION

In Vitro Antioxidant Activity. To evaluate the antioxidant activity of the selenium-containing CQ derivatives, the oxygen radical absorbance capacity assay using fluorescein (ORAC-FL) was employed, and Trolox (6-hydroxy-2,5,7,8-tetramethylchroman-2-carboxylic acid), a vitamin E analogue, was used as an internal standard to which the unit value is arbitrarily given.[40,41] As shown in Table 1, the target compounds demonstrated better antioxidant activity (ORAC-FL values of 1.53−1.96 Trolox equivalents) than CQ (ORAC-FL value 0.62). Specifically, the results indicated that compounds **8a**, **8b**, and **8d** exhibited best antioxidant activity with 1.94, 1.95, and 1.96 Trolox equivalents, respectively, and thus they could be considered as potent antioxidant agents.

Hydrogen Peroxide Scavenging Activity. The removal of ROS, such as hydrogen peroxide, is especially important in the elderly and AD patients.[15,42,43] To further evaluate the antioxidant activity of the selenium-containing CQ derivatives, compounds **8a**, **8b**, and **8d** were analyzed using the horseradish peroxidase assay (HRPA);[44] CQ and M30 were used as reference compounds. The results in Figure 2 indicate that all compounds showed significantly better scavenging activities for hydrogen peroxide compared to CQ. Compounds **8a**, **8b**, and **8d** exhibited full scale scavenging activities for hydrogen peroxide at high concentrations of 150−200 μM, but **8a** (100 μM, 62% scavenging; 80 μM, 35%; 50 μM, 17%) demonstrated higher scavenging activity than **8b** (100 μM, 44%; 80 μM, 17%; 50 μM, 7%) and **8d** (100 μM, 40%; 80 μM, 26%; 50 μM, 10%)

dx.doi.org/10.1021/cn500119g | ACS Chem. Neurosci. 2014, 5, 952−962

Table 1. Oxygen Radical Absorbance Capacity by Fluorescence (ORAC-FL, Trolox Equivalents) of Selenium-Containing CQ Derivatives 8a−8i

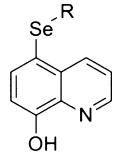

8a-8i

Compd	R	ORAC ± SD [a]
8a	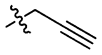	1.94 ± 0.04
8b	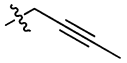	1.95 ± 0.13
8c	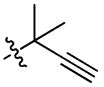	1.54 ± 0.21
8d		1.96 ± 0.07
8e	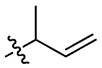	1.67 ± 0.19
8f		1.61 ± 0.11
8g	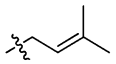	1.53 ± 0.15
8h	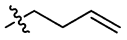	1.68 ± 0.21
8i	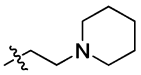	1.78 ± 0.18
CQ	-	0.62 ± 0.01
M30	-	5.77 ± 0.32

[a]The mean ± SD of three independent experiments. Data are expressed as μmole of Trolox equivalent/μmol of tested compound.

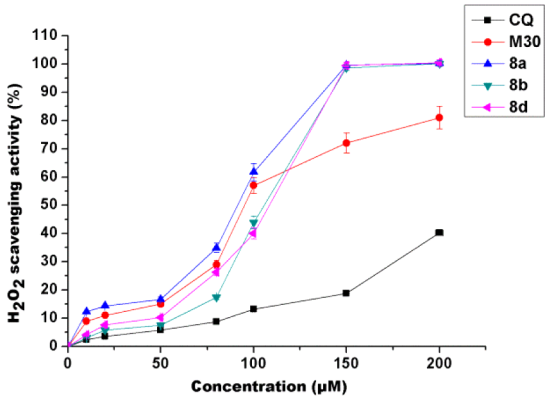

Figure 2. Hydrogen peroxide scavenging activity of **8a**, **8b**, **8d**, CQ, and M30 in the HRPA assay (H_2O_2 = 100 μM). Values reported are means ± SD of three independent experiments.

at lower concentrations. In contrast, CQ (150 μM, 19%; 200 μM, 40%) and M30 (150 μM, 71%; 200 μM, 80%) possess extremely weak and moderate activity even at high concentrations, respectively.

Intracellular Antioxidant Assay. The intracellular antioxidant activity of **8a** in human SH-SY5Y cells was evaluated in a cellular antioxidant assay using dichlorofluorescein diacetate (DCFH-DA)[45,46] with CQ and Trolox as the reference compounds. As reported in Figure 3A, **8a** (1 μM, 103% cell viability; 5 μM, 100%; 10 μM, 100%; 25 μM, 78%; 50 μM, 43%) did not affect the cell viability at 10 μM; thus, the maximum concentration used in the subsequent assay was 10 μM. Figure 3B shows the concentration-dependent protective effect of compounds against *tert*-butyl hydroperoxide induced intracellular oxidative stress. Trolox (5 μM, 95% of control; 10 μM, 88%; 20 μM, 80%) and the tested compounds exhibited antioxidant activity, and **8a** (2.5 μM, 87%; 5 μM, 84%; 10 μM, 76%) had higher potency than CQ (2.5 μM, 98%; 5 μM, 96%; 10 μM, 93%). These data further suggest the potential of **8a** as an efficient multifunctional anti-AD agent that exhibits intracellular antioxidant activity.

Metal-Chelating Properties of Compound 8a. The ability of **8a** to binding biometals such as Cu(II), Zn(II), Fe(II), and Fe(III) was investigated by UV−vis spectrometry, and the results are shown in Figure 4.[47−52] As shown in Figure 4A, new optical bands appeared when $CuSO_4$, $ZnCl_2$, or $FeSO_4$ was added to a solution containing **8a**; that is, the maximum absorption (242 nm) shifted to 279, 279, or 259 nm, respectively. Upon the addition of Cu^{2+}, a new band associated with the copper complex appeared at 415 nm. These results suggest that **8a** is able to interact with Cu(II), Zn(II), and Fe(II). However, upon addition of $FeCl_3$, a decrease in absorption was observed, rather than a significant shift, thereby indicating a possible interaction between **8a** and Fe(III). The binding stoichiometry of **8a** with Cu^{2+} was determined by measuring the changes in absorption at 415 nm when **8a** was titrated with Cu^{2+}, as depicted in Figure 4B. The presence of an isosbestic point revealed the formation of a unique Cu^{2+}−**8a** complex (Figure 4B), and the titration analysis was consistent with a 1:2 Cu^{2+}/ligand molar ratio (Figure 4B, inset).

Prevention of Copper-Based Redox Activity in the Presence of 8a. An increasing number of studies have indicated that excessive free radical generation may trigger neuronal cell death in AD patients.[15] Under oxidative stress, the neurotoxicity of Aβ was caused by the generation of ROS, including $OH^{\bullet}$ and $O_2^{\bullet-}$.[53] The effect of compound **8a** on the Cu−ascorbate redox system (Scheme 2)[54−58] was evaluated due to redox-active Cu(II) being implicated in the pathways of ROS production. The results in Figure 5 present that $OH^{\bullet-}$ produced by copper and ascorbate increased sharply with time and then stagnated at nearly 14 min. Interestingly, this process was completely inhibited by **8a** and M30, which suggested that both **8a** and M30 were capable of preventing copper redox cycling.

Inhibition of Cu^{2+}-Induced Aβ Aggregation by 8a. To investigate the effects of the selenium-containing CQ derivatives to inhibit Cu(II)-induced $A\beta_{1-42}$ aggregation, we analyzed **8a** using thioflavin T (ThT) fluorescence and transmission electron microscopy (TEM) (Figure 6), which depicts Aβ aggregate morphology. CQ was used as a positive control because it is known to attenuate metal ion-Aβ aggregation. The $A\beta_{1-42}$ peptide (25 μM) was treated with Cu^{2+} (25 μM) for 2 min at room temperature followed by

dx.doi.org/10.1021/cn500119g | ACS Chem. Neurosci. 2014, 5, 952−962

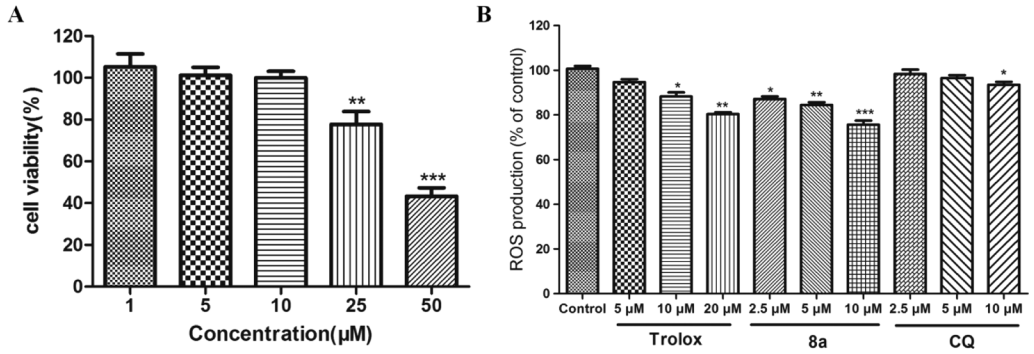

Figure 3. (A) Effect of **8a** on cell viability in SH-SY5Y cells. (B) Intracellular ROS induced by exposure to *t*-BuOOH without or with compounds measured using DCFH-DA. The results are reported as the mean of three independent experiments performed in sextuplicate. Statistical significance was analyzed using ANOVA: $*p < 0.05$, $**p < 0.01$, $***p < 0.001$, versus control.

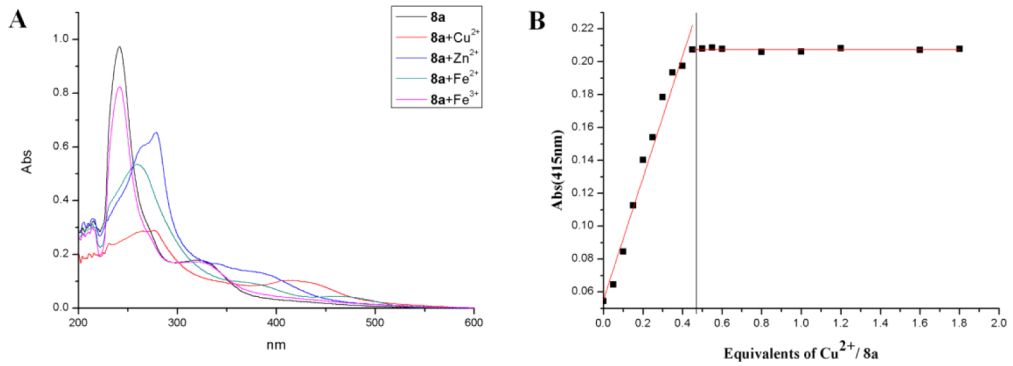

Figure 4. (A) UV spectrum of **8a** (50 μM) alone and in the presence of $CuSO_4$ (50 μM), $ZnCl_2$ (50 μM), or $FeSO_4$ (50 μM) in buffer (20 mM HEPES, 150 mM NaCl, pH 7.4). (B) UV−vis titration of **8a** with Cu^{2+} in buffer (20 mM HEPES, 150 mM NaCl, pH 7.4) at room temperature. The concentrations of Cu^{2+} and **8a** were 0−144 and 80 μM, respectively. A breakpoint is observed at [Cu^{2+}]:[**8a**] = 0.5:1.

Scheme 2. Redox Cycling of Copper in the Presence of Oxygen and Ascorbate to Produce OH·

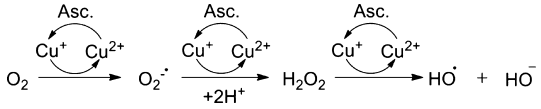

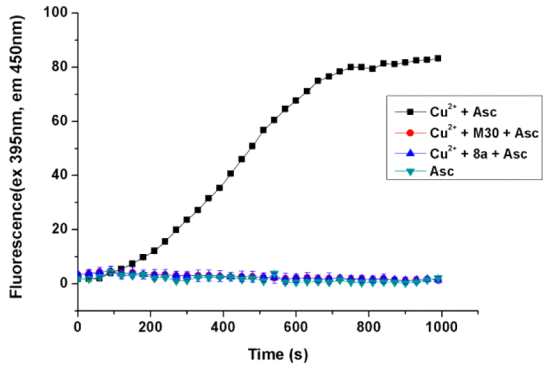

Figure 5. Fluorescence intensity of 7-hydroxy-coumarin-3-carboxylic acid (CCA) after incubation of CCA (50 μM) and ascorbate (150 μM) with Cu^{2+} (5 μM). **8a** and M30 (15 μM) was added at $t = 0$ s, prior to Cu^{2+}. Asc is a negative control with buffer and ascorbate only. All solutions were dissolved and diluted in KH_2PO_4/NaCl [20 mM] buffer containing desferryl [1 μM] except $CuSO_4$ (dissolved in Milli-Q water only). Values reported are the means ± SD of three independent experiments.

incubation with or without a chelator (50 μM) for 24 h at 37 °C. Cu^{2+}-induced Aβ aggregation was modulated by treatment with **8a** as indicated in Figure 6A. The fluorescence of Aβ treated with Cu^{2+} is 160% that of Aβ alone, which demonstrates that Cu^{2+} accelerates Aβ aggregation. Conversely, the fluorescence of Aβ treated with Cu^{2+} and the chelator decreased dramatically (**8a**, 69% inhibition; CQ, 68% inhibition; M30, 68% inhibition). The TEM images in Figure 6B are consistent with the ThT binding assay. Aβ fibrils in the presence of Cu(II) (Figure 6Bc) showed more definition than with Aβ alone (Figure 6Bb), and fewer Aβ fibrils were observed upon addition of **8a** (Figure 6Be).

Disaggregation of Metal-Induced Aβ_{1-42} Aggregation Fibrils by 8a. To study the disaggregation of metal-induced Aβ_{1-42} aggregates, a chelator (50 μM) was added to Aβ fibrils generated by reacting Aβ_{1-42} (25 μM) with 1.0 equiv of Cu^{2+} (25 μM) for 24 h at 37 °C with constant agitation. TEM images showed that well-structured Aβ_{1-42} fibrils were formed in the presence of Cu(II) (Figure 7Bb). Incubation of the Aβ_{1-42} fibrils with CQ (Figure 7Bc), **8a** (Figure 7Bd), or M30 (Figure 7Be) for 24 h resulted in the disassembly of the Aβ_{1-42} fibrils.

In Vitro Blood-Brain Barrier Permeation Assay. Blood-brain barrier (BBB) penetration is the first requirement for successful CNS drugs as they are destined to act within the central nervous system. To explore whether the selenium-containing CQ compounds would be able to penetrate into the brain, a parallel artificial membrane permeation assay was modified for the blood-brain barrier (PAMPA-BBB), as recently described by Di et al.[59] The in vitro permeabilities (P_e) of newly synthesized compounds **8a**−**8i** and 13 commercial drugs

dx.doi.org/10.1021/cn500119g | ACS Chem. Neurosci. 2014, 5, 952−962

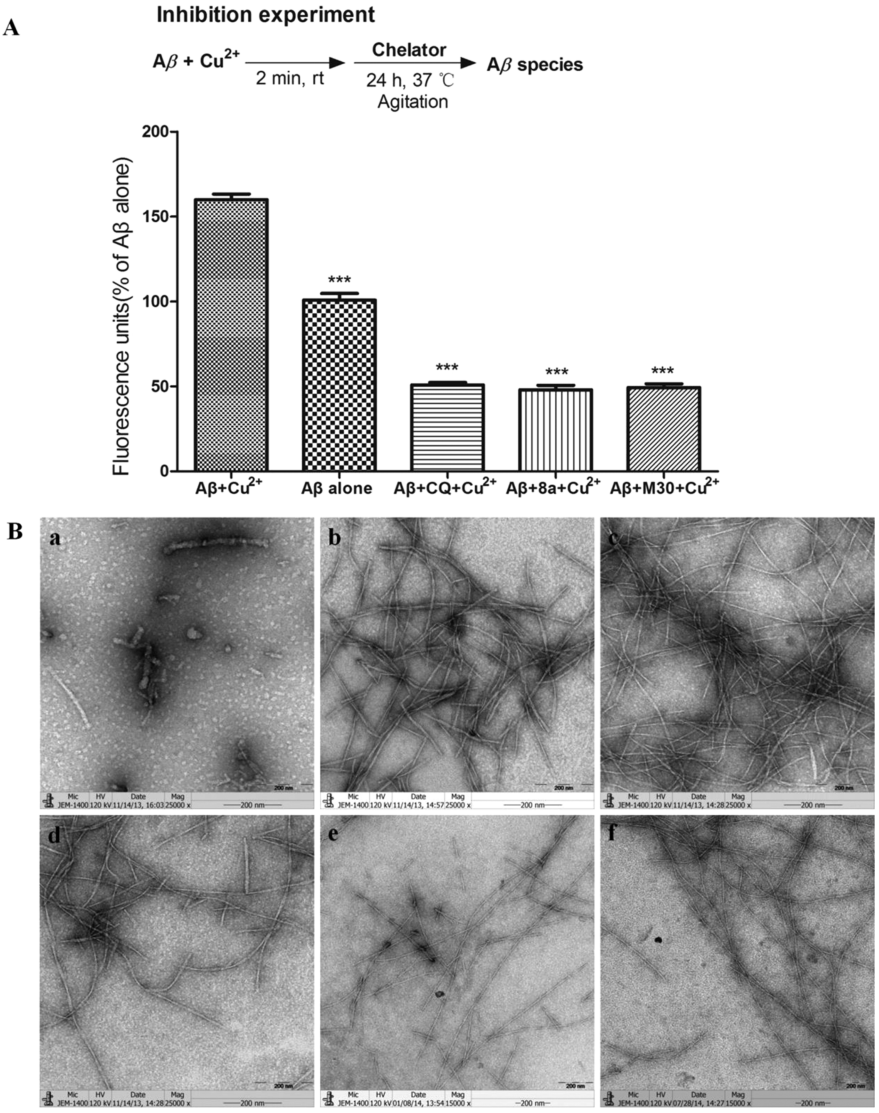

Figure 6. (A) Top: Scheme of the inhibition experimental procedure. Bottom: Results of the ThT binding assay. Statistically significant differences from $A\beta_{1-42}$ + Cu^{2+} were analyzed by ANOVA: ***$p < 0.001$. (B) TEM images showing the inhibition of Cu(II)-induced $A\beta_{1-42}$ aggregation ([$A\beta_{1-42}$] = 25 μM, [**8a**] = 50 μM, [CQ] = 50 μM, [M30] = 50 μM, [Cu^{2+}] = 25 μM, 37 °C, 24 h; (a) $A\beta_{1-42}$, 0 h; (b) $A\beta_{1-42}$ alone; (c) $A\beta_{1-42}$ + Cu^{2+}, (d) $A\beta_{1-42}$ + Cu^{2+} + CQ; (e) $A\beta_{1-42}$ + Cu^{2+} + **8a**; (f) $A\beta_{1-42}$ + Cu^{2+} + M30).

through a lipid extract of porcine brain were determined using a mixture of of PBS and ethanol in the ratio of 70:30 (Table S1, Supporting Information). A plot of experimental data versus reported values produced the linear correlation P_e (exp) = 1.4574P_e (bibil) − 1.0773 (R^2 = 0.9427) (see Supporting Information Figure S1). According to this equation and taking into account the described limits by Di et al. for BBB permeation, we determined that compounds with permeability above 4.7 × 10^{-6} cm/s penetrate into the CNS by passive diffusion (see Supporting Information Table S2). Analysis of the target compounds in the PAMPA-BBB assay indicated that all of the compounds showed permeability values over this limit (Table 2), demonstrating that all compounds could cross the BBB and thus can potentially reach their biological targets within the CNS. The structure−activity relationship study showed that compounds **8a**−**8c**, which bear alkynyl groups on the oxine, had much higher permeability; however, for compounds with alkenyl groups, such as **8d**−**8h**, the permeabilities were slightly lower. It is worth noting that compound **8i**, which contains a piperidine group on the oxine moiety, showed outstanding permeability (P_e = 27.45 × 10^{-6} cm/s).

CONCLUSIONS

A new series of multitarget-directed selenium-containing CQ derivatives were developed as lead compounds for the treatment of AD. Among the synthesized compounds, **8a** exhibited metal-chelating ability, significant inhibition of Cu(II)-induced $A\beta_{1-42}$ aggregation, disaggregation of $A\beta$ fibrils generated by Cu(II)-induced $A\beta$ aggregation, H_2O_2 and intracellular antioxidant activity, and prevention of copper redox cycling. **8a** was also capable of crossing the BBB in a parallel artificial membrane permeation assay. Based on these results, **8a** is a promising multifunctional candidate for the treatment of AD. Further investigations of AD therapeutic candidates based on these results are in progress.

METHODS

General Remarks. NMR spectra were recorded using TMS as the internal standard on a Bruker Avance III spectrometer at 400.132 (^{1}H

dx.doi.org/10.1021/cn500119g | ACS Chem. Neurosci. 2014, 5, 952−962

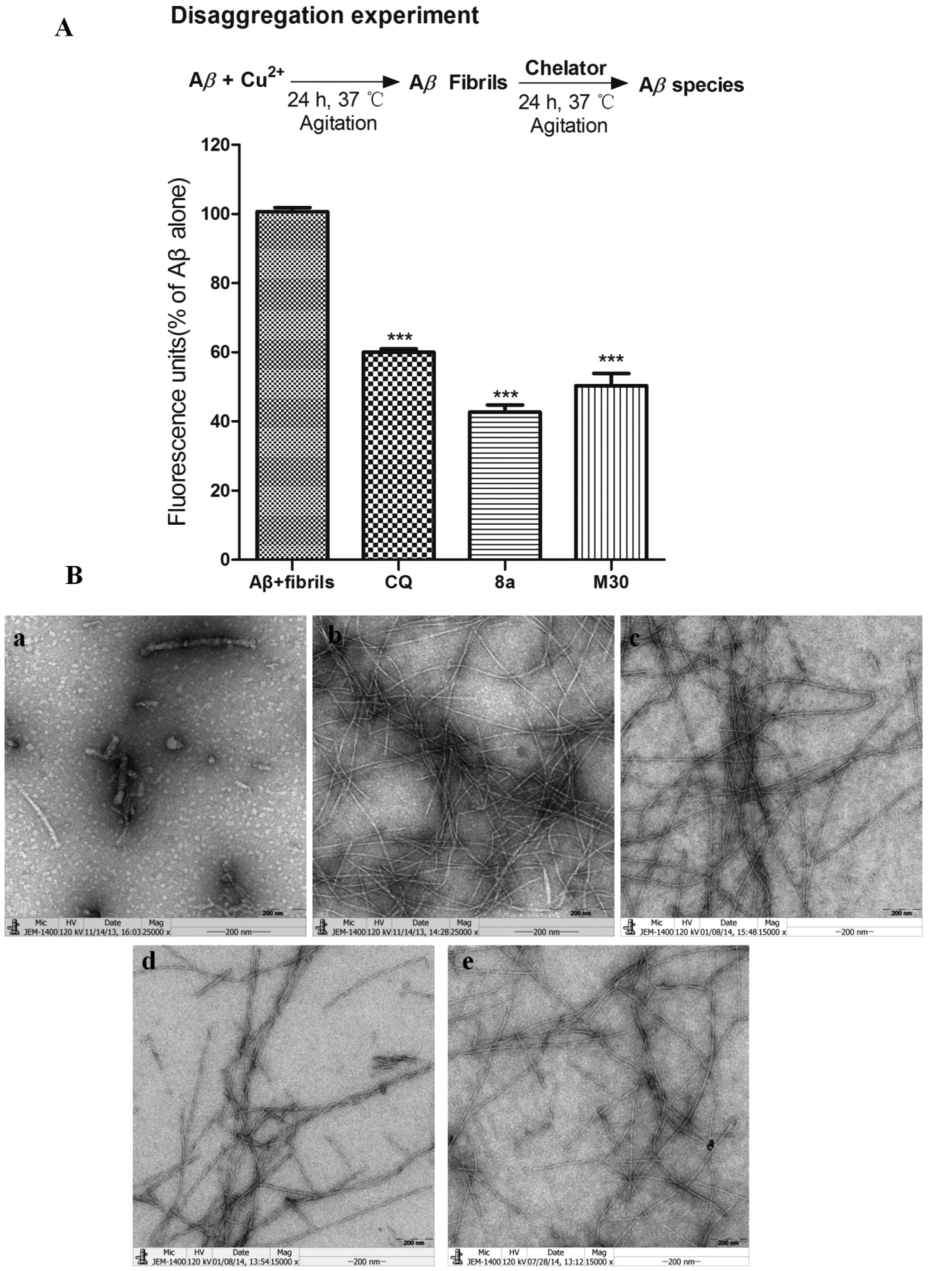

Figure 7. (A) Top: Scheme of the disaggregation experimental procedure. Bottom: Results of the ThT binding assay. Statistically significant differences from control were analyzed by ANOVA: ***$p < 0.001$. (B) TEM images ([Aβ_{1-42}] = 25 μM, [**8a**] = 50 μM, [CQ] = 50 μM, [M30] = 50 μM, [Cu^{2+}] = 25 μM, 37 °C, 24 h; (a) Aβ_{1-42}, 0 h, (b) Aβ_{1-42} + Cu^{2+}, (c) Aβ_{1-42} + Cu^{2+} + CQ, (d) Aβ_{1-42} + Cu^{2+} + **8a**, (e) Aβ_{1-42} + Cu^{2+} + M30).

NMR) and 100.614 (^{13}C NMR) MHz. MS spectra were obtained on an Agilent LC−MS 6120 instrument with an ESI and APCI mass selective detector. The melting points were determined using an SRS-Opti Melt automated melting point instrument. The reactions were monitored by thin-layer chromatography (TLC). Flash column chromatography was performed using silica gel (200−300 mesh) purchased from Qingdao Haiyang Chemical Co. Ltd. The high-resolution mass spectra were obtained using a LTQ Orbitrap XL (Thermo Scientific) mass spectrometer. The purity (≥95%) of the samples was determined by HPLC, conducted on a Shimadzu LC-20AT series system, TC-C18 column (4.6 × 250 mm, 5 μm), eluted with CH_3OH/H_2O, 70/30, at a flow rate of 0.5 mL/min.

Synthesis of 2 and 3. **2** and **3** were synthesized according to a previously described method.[37−39]

*5-Nitroquinolin-8-ol (**2**).* Yellow solid, 80% yield. ^{1}H NMR (400 MHz, DMSO) δ 9.14 (d, J = 8.8 Hz, 1H), 9.02 (d, J = 3.5 Hz, 1H), 8.54 (d, J = 8.7 Hz, 1H), 7.88 (dd, J = 8.7, 3.9 Hz, 1H), 7.21 (d, J = 8.8 Hz, 1H).

*tert-Butyl (5-Nitroquinolin-8-yl) Carbonate (**3**).* Yellow solid, 94% yield. ^{1}H NMR (400 MHz, $CDCl_3$) δ 9.06 (d, J = 8.9 Hz, 1H), 9.03 (s, 1H), 8.44 (d, J = 8.4 Hz, 1H), 7.68 (dd, J = 5.5, 3.3 Hz, 1H), 7.62 (d, J = 8.4 Hz, 1H), 1.60 (s, 9H).

*Synthesis of 5-Aminoquinolin-8-yl tert-Butyl Carbonate (**4**).* To a solution of *tert*-butyl (5-nitroquinolin-8-yl) carbonate (**3**) (14.0 g, 66.8 mmol) in 200 mL of ethyl acetate was added 8.0 equiv (120 g, 535.1 mmol) of $SnCl_2 \cdot 2H_2O$ in portions. After the reaction was stirred at room temperature for 3 h, saturated $NaHCO_3$ was added to pH 8. The organic phase was separated and the aqueous phase was extracted with ethyl acetate. The combined organic phase was washed with brine, dried over anhydrous Na_2SO_4, and evaporated to obtain the pure product as a yellow solid. 78% yield. R_f = 0.32 (CH_2Cl_2/CH_3OH = 20/1). ^{1}H NMR (400 MHz, $CDCl_3$) δ 8.90 (s, 1H), 8.20−8.05 (m,

dx.doi.org/10.1021/cn500119g | ACS Chem. Neurosci. 2014, 5, 952−962

Table 2. Permeability ($P_e \times 10^{-6}$ cm/s), As Determined by the PAMPA-BBB Assay and Predicted CNS Penetration of the Target Compounds

compd	P_e ($\times 10^{-6}$ cm/s)[a]	prediction
8a	18.94 ± 0.32	CNS+
8b	18.26 ± 1.80	CNS+
8c	19.30 ± 0.94	CNS+
8d	16.97 ± 0.96	CNS+
8e	8.90 ± 1.37	CNS+
8f	8.56 ± 0.90	CNS+
8g	6.58 ± 0.65	CNS+
8h	8.11 ± 1.14	CNS+
8i	27.45 ± 2.16	CNS+
chlorpromazine	6.00 ± 0.30	CNS+

[a]Compounds were dissolved in DMSO at 5 mg mL^{-1} and diluted with PBS/EtOH (70:30). Values are expressed as the means ± SD of three independent experiments.

1H), 7.38–7.29 (m, 2H), 6.72 (dd, *J* = 7.9, 3.4 Hz, 1H), 4.12 (s, 2H), 1.59 (s, 9H). LC/MS (ESI): 261.1 $[M + H]^+$.

*Synthesis of tert-Butyl (5-Selenocyanatoquinolin-8-yl) Carbonate (**5**).* To a cold solution (20 mL, −5 °C) of 10% HCl was added 2.0 g of 5-aminoquinolin-8-yl *tert*-butyl carbonate (**4**). Sodium nitrite (0.64 g, 1.2 equiv) was added with stirring, and the reaction mixture was kept at −3 °C. Upon completion of the reaction, saturated sodium acetate was added to pH 6.0. Potassium selenocyanate (1.7 g, 1.5 equiv) in water (6 mL) was added dropwise. The resulting frothy orange solution was allowed to stand for 1 h, and the mixture was extracted with ethyl acetate, washed with brine, and dried over anhydrous Na_2SO_4. The solvent was evaporated under reduced pressure, and the product was purified by silica-column chromatography to afford a yellow solid. 56% yield. R_f = 0.44 (petroleum/EtOAc = 3/1). ^{1}H NMR (400 MHz, $CDCl_3$) δ 9.04–9.00 (m, 1H), 8.59 (d, *J* = 8.6 Hz, 1H), 8.10 (dd, *J* = 7.9, 0.6 Hz, 1H), 7.65 (ddd, *J* = 8.6, 4.1, 0.6 Hz, 1H), 7.57 (dd, *J* = 7.9, 0.6 Hz, 1H), 1.60 (s, 9H). LC/MS (ESI): 351.0 $[M + H]^+$.

*Synthesis of Di-tert-butyl (5,5′-Diselanediylbis(quinoline-8,5-diyl)) Dicarbonate (**6**).* *tert*-Butyl (5-selenocyanatoquinolin-8-yl) carbonate (**5**, 150 mg) was added to potassium hydroxide (60 mg, 1.5 equiv) in methanol (4 mL), affording an orange-yellow precipitate that was swirled vigorously. The mixture was allowed to stand for 15 min. Water (30 mL) was added, and the pH was adjusted to 8.0 using 10% HCl. The mixture was extracted with CH_2Cl_2, washed with brine, and dried over anhydrous Na_2SO_4, and the solvent was then evaporated under reduced pressure. The product was purified by silica-column chromatography to yield a yellow solid. 74% yield. R_f = 0.37 (petroleum/EtOAc = 5/1). ^{1}H NMR (400 MHz, $CDCl_3$) δ 8.83 (dd, *J* = 4.1, 1.5 Hz, 2H), 8.22 (dd, *J* = 8.6, 1.5 Hz, 2H), 7.75 (d, *J* = 7.8 Hz, 2H), 7.34 (d, *J* = 7.8 Hz, 2H), 7.22 (dd, *J* = 8.6, 4.2 Hz, 2H), 1.61 (s, 18H). LC/MS (ESI): 649.0 $[M + H]^+$.

General Procedure for the Synthesis of 7a–7i. $NaBH_4$ (53 mg, 6.0 equiv) was added in portions to diselenide **6** (150 mg, 1.0 equiv) in ethanol/water (1/1, 8 mL), and the mixture was stirred for 10–15 min. The corresponding alkyl halide (2.0 equiv) was added and the reaction was stirred at room temperature for 1 h. Water was added, and the mixture was extracted with CH_2Cl_2. The organic phase was washed with brine and dried over anhydrous Na_2SO_4. The solvent was evaporated, and the products were purified using a silica gel column.

*tert-Butyl (5-(Prop-2-yn-1-ylselanyl)quinolin-8-yl) Carbonate (**7a**).* Yellow oil, 67% yield. R_f = 0.43 (petroleum/EtOAc = 5/1). ^{1}H NMR (400 MHz, $CDCl_3$) δ 8.94 (dd, *J* = 4.1, 1.5 Hz, 1H), 8.77 (dd, *J* = 8.6, 1.5 Hz, 1H), 8.00 (d, *J* = 7.8 Hz, 1H), 7.51 (dd, *J* = 8.3, 3.9 Hz, 1H), 7.49 (d, *J* = 7.7 Hz, 1H), 3.45 (d, *J* = 2.7 Hz, 2H), 2.20 (t, *J* = 2.7 Hz, 1H), 1.60 (s, 9H). LC/MS (ESI): 364.0 $[M + H]^+$.

*5-(But-2-yn-1-ylselanyl)quinolin-8-yl tert-Butyl Carbonate (**7b**).* Yellow oil, 72% yield. R_f = 0.39 (petroleum/EtOAc = 5/1). ^{1}H NMR (400 MHz, $CDCl_3$) δ 8.93 (d, *J* = 4.1 Hz, 1H), 8.78 (d, *J* = 8.6 Hz, 1H), 7.97 (d, *J* = 7.8 Hz, 1H), 7.52–7.46 (m, 2H), 3.46 (dd, *J* = 4.6, 2.1 Hz, 2H), 1.69 (t, *J* = 2.1 Hz, 3H), 1.60 (s, 9H). LC/MS (ESI): 378.0 $[M + H]^+$.

*tert-Butyl (5-((2-Methylbut-3-yn-2-yl)selanyl)quinolin-8-yl) Carbonate (**7c**).* Yellow oil, 64% yield. R_f = 0.41 (petroleum/EtOAc = 5/1). ^{1}H NMR (400 MHz, $CDCl_3$) δ 8.92 (dd, *J* = 4.1, 1.5 Hz, 1H), 8.68 (dd, *J* = 8.5, 1.5 Hz, 1H), 7.89 (d, *J* = 7.8 Hz, 1H), 7.49 (dd, *J* = 8.6, 4.2 Hz, 1H), 7.46 (d, *J* = 7.9 Hz, 1H), 5.82 (dt, *J* = 5.1, 2.5 Hz, 1H), 1.60 (s, 9H), 1.39 (d, *J* = 2.5 Hz, 6H). LC/MS (ESI): 392.1 $[M + H]^+$.

*5-(Allylselanyl)quinolin-8-yl tert-Butyl Carbonate (**7d**).* Yellow oil, 69% Yield. R_f = 0.42 (petroleum/EtOAc = 5/1). ^{1}H NMR (400 MHz, $CDCl_3$) δ 8.93 (dd, *J* = 4.1, 1.4 Hz, 1H), 8.75 (dd, *J* = 8.6, 1.5 Hz, 1H), 7.85 (d, *J* = 7.8 Hz, 1H), 7.50 (dd, *J* = 8.6, 4.1 Hz, 1H), 7.45 (d, *J* = 7.8 Hz, 1H), 5.95–5.82 (m, 1H), 4.85 (dd, *J* = 9.9, 0.5 Hz, 1H), 4.80 (d, *J* = 16.9 Hz, 1H), 3.52–3.45 (m, 2H), 1.59 (s, 9H). LC/MS (ESI): 366.1 $[M + H]^+$.

*5-(But-3-en-2-ylselanyl)quinolin-8-yl tert-Butyl Carbonate (**7e**).* Yellow oil, 73% yield. R_f = 0.41 (petroleum/EtOAc = 5/1). ^{1}H NMR (400 MHz, $CDCl_3$) δ 8.91 (dd, *J* = 4.1, 1.4 Hz, 1H), 8.81 (dd, *J* = 8.5, 1.2 Hz, 1H), 7.88 (d, *J* = 7.8 Hz, 1H), 7.46 (ddd, *J* = 11.1, 8.0, 4.6 Hz, 3H), 5.86 (ddd, *J* = 17.1, 10.0, 8.4 Hz, 1H), 4.70 (dd, *J* = 31.5, 13.6 Hz, 2H), 3.89–3.77 (m, 1H), 1.59 (s, 9H), 1.45 (d, *J* = 6.9 Hz, 3H). LC/MS (ESI): 380.1 $[M + H]^+$.

*tert-Butyl (5-((2-Methylallyl)selanyl)quinolin-8-yl) Carbonate (**7f**).* Yellow oil, 75% Yield. R_f = 0.45 (petroleum/EtOAc = 5/1). ^{1}H NMR (400 MHz, $CDCl_3$) δ 8.92 (dd, *J* = 4.1, 1.6 Hz, 1H), 8.75 (dd, *J* = 8.6, 1.5 Hz, 1H), 7.83 (d, *J* = 7.8 Hz, 1H), 7.48 (dd, *J* = 8.6, 4.1 Hz, 1H), 7.44 (d, *J* = 7.8 Hz, 1H), 4.63–4.59 (m, 1H), 4.45 (s, 1H), 3.47 (s, 2H), 1.86 (s, 3H), 1.59 (s, 9H). LC/MS (ESI): 380.1 $[M + H]^+$.

*tert-Butyl (5-((3-Methylbut-2-en-1-yl)selanyl)quinolin-8-yl) Carbonate (**7g**).* Yellow oil, 77% yield. R_f = 0.38 (petroleum/EtOAc = 5/1). ^{1}H NMR (400 MHz, $CDCl_3$) δ 8.83 (dd, *J* = 4.1, 1.4 Hz, 1H), 8.68 (dd, *J* = 8.6, 1.4 Hz, 1H), 7.77 (d, *J* = 7.8 Hz, 1H), 7.38 (dd, *J* = 8.6, 4.1 Hz, 1H), 7.35 (d, *J* = 7.8 Hz, 1H), 5.22 (t, *J* = 8.3 Hz, 1H), 3.40 (d, *J* = 8.3 Hz, 2H), 1.51 (s, 9H), 1.46 (s, 3H), 1.11 (s, 3H). LC/MS (ESI): 394.1 $[M + H]^+$.

*5-(But-3-en-1-ylselanyl)quinolin-8-yl tert-Butyl Carbonate (**7h**).* Yellow oil, 71% Yield. R_f = 0.40 (petroleum/EtOAc = 5/1). ^{1}H NMR (400 MHz, $CDCl_3$) δ 8.93 (d, *J* = 4.1 Hz, 1H), 8.74 (d, *J* = 8.6 Hz, 1H), 7.87 (d, *J* = 7.8 Hz, 1H), 7.50 (dd, *J* = 8.6, 4.1 Hz, 1H), 7.45 (d, *J* = 7.8 Hz, 1H), 5.79 (ddt, *J* = 16.9, 10.4, 6.5 Hz, 1H), 5.05 (dd, *J* = 13.5, 5.1 Hz, 2H), 2.94 (t, *J* = 7.4 Hz, 2H), 2.40 (dd, *J* = 14.1, 7.0 Hz, 2H), 1.60 (s, 9H). LC/MS (ESI): 380.1 $[M + H]^+$.

*tert-Butyl (5-((2-(Piperidin-1-yl)ethyl)selanyl)quinolin-8-yl) Carbonate (**7i**).* Yellow oil, 56% yield. R_f = 0.25 (petroleum/EtOAc = 5/1). ^{1}H NMR (400 MHz, $CDCl_3$) δ 8.92 (dd, *J* = 4.1, 1.4 Hz, 1H), 8.73 (dd, *J* = 8.6, 1.3 Hz, 1H), 7.85 (d, *J* = 7.8 Hz, 1H), 7.48 (dd, *J* = 8.6, 4.1 Hz, 1H), 7.44 (d, *J* = 7.8 Hz, 1H), 3.02 (dd, *J* = 8.5, 6.6 Hz, 2H), 2.63–2.59 (m, 2H), 2.35 (s, 4H), 1.59 (s, 9H), 1.53 (dt, *J* = 11.0, 5.7 Hz, 6H). LC/MS (ESI): 437.1 $[M + H]^+$.

General Procedure for the Synthesis of 8a–8i. Piperidine (1.5 equiv) was added to a solution of **7** (1.0 equiv) in anhydrous DCM (4 mL) at ambient temperature. Upon completion of the reaction, the solvent was evaporated under reduced pressure and the crude product was purified by silica-column chromatography to yield the target product.

*5-(Prop-2-yn-1-ylselanyl)quinolin-8-ol (**8a**).* Yellow solid, 72% yield. Mp 82.5–83.1 °C. R_f = 0.25 (CH_2Cl_2/CH_3OH = 20/1). ^{1}H NMR (400 MHz, $CDCl_3$) δ 8.84–8.78 (m, 2H), 7.98 (d, *J* = 7.9 Hz, 1H), 7.54 (dd, *J* = 8.5, 4.2 Hz, 1H), 7.14 (d, *J* = 7.9 Hz, 1H), 3.38–3.34 (m, 2H), 2.16 (t, *J* = 2.7 Hz, 1H). ^{13}C NMR (101 MHz, $CDCl_3$) δ 152.78, 147.01, 137.85, 137.13, 136.14, 129.77, 121.64, 115.24, 109.14, 79.77, 71.30, 12.57. $[M + H]^+$ for $C_{12}H_{10}NOSe$ pred. 263.9922, meas. 263.9921; HPLC purity: 98.68%.

*5-(But-2-yn-1-ylselanyl)quinolin-8-ol (**8b**).* Yellow solid, 65% yield. Mp 97.8–98.9 °C. R_f = 0.23 (CH_2Cl_2/CH_3OH = 20/1). ^{1}H NMR (400 MHz, $CDCl_3$) δ 8.82 (dd, *J* = 8.5, 1.5 Hz, 1H), 8.79 (dd, *J* = 4.2, 1.5 Hz, 1H), 7.95 (d, *J* = 7.9 Hz, 1H), 7.53 (dd, *J* = 8.5, 4.2 Hz, 1H), 7.13 (d, *J* = 7.9 Hz, 1H), 3.39–3.33 (m, 2H), 1.68 (t, *J* = 2.6 Hz, 3H).

dx.doi.org/10.1021/cn500119g | ACS Chem. Neurosci. 2014, 5, 952–962

^{13}C NMR (101 MHz, $CDCl_3$) δ 153.63, 147.94, 138.78, 137.92, 137.35, 130.92, 122.30, 116.84, 110.25, 80.58, 75.77, 14.85, 3.65. $[M + H]^+$ for $C_{13}H_{12}NOSe$ pred. 278.0079, meas. 278.0080; HPLC purity: 99.32%.

*5-((2-Methylbut-3-yn-2-yl)selanyl)quinolin-8-ol (**8c**).* Yellow solid, yield 68%. Mp 107.4−108.2 °C. R_f = 0.21 (CH_2Cl_2/CH_3OH = 20/1). ^{1}H NMR (400 MHz, $CDCl_3$) δ 8.77 (d, J = 3.0 Hz, 1H), 8.69 (d, J = 8.4 Hz, 1H), 7.85 (d, J = 7.9 Hz, 1H), 7.51 (dd, J = 8.4, 4.1 Hz, 1H), 7.11 (d, J = 7.8 Hz, 1H), 5.77 (dd, J = 3.2, 1.6 Hz, 1H), 1.33 (d, J = 2.4 Hz, 6H). ^{13}C NMR (101 MHz, $CDCl_3$) δ 153.38, 147.83, 137.46, 137.26, 130.58, 122.36, 116.77, 110.01, 101.17, 97.15, 77.92, 29.66, 19.74. $[M + H]^+$ for $C_{14}H_{14}NOSe$ pred. 292.0235, meas. 292.0234; HPLC purity: 97.63%.

*5-(Allylselanyl)quinolin-8-ol (**8d**).* Yellow solid, yield 64%. Mp 52.7−53.3 °C. R_f = 0.26 (CH_2Cl_2/CH_3OH = 20/1). ^{1}H NMR (400 MHz, $CDCl_3$) δ 8.84−8.71 (m, 2H), 7.83 (d, J = 7.9 Hz, 1H), 7.52 (dd, J = 8.5, 4.2 Hz, 1H), 7.11 (d, J = 7.9 Hz, 1H), 5.87 (ddt, J = 17.6, 9.9, 7.7 Hz, 1H), 4.78 (dd, J = 9.9, 0.5 Hz, 1H), 4.68 (dd, J = 16.9, 1.2 Hz, 1H), 3.42−3.35 (m, 2H). ^{13}C NMR (101 MHz, $CDCl_3$) δ 153.24, 147.88, 138.85, 137.74, 137.25, 134.37, 130.80, 122.38, 116.74, 116.64, 110.22, 31.97. $[M + H]^+$ for $C_{12}H_{12}NOSe$ pred. 266.0079, meas. 266.0077; HPLC purity: 96.45%.

*5-(But-3-en-2-ylselanyl)quinolin-8-ol (**8e**).* Yellow solid, yield 71%. Mp 45.9−46.5 °C. R_f = 0.24 (CH_2Cl_2/CH_3OH = 20/1). ^{1}H NMR (400 MHz, $CDCl_3$) δ 8.80 (dd, J = 8.5, 1.5 Hz, 1H), 8.77 (dd, J = 4.2, 1.4 Hz, 1H), 7.83 (d, J = 7.9 Hz, 1H), 7.51 (dd, J = 8.5, 4.2 Hz, 1H), 7.11 (d, J = 7.9 Hz, 1H), 5.86 (ddd, J = 17.0, 10.1, 8.3 Hz, 1H), 4.71 (d, J = 10.1 Hz, 1H), 4.61 (d, J = 17.0 Hz, 1H), 3.85−3.66 (m, 1H), 1.43 (d, J = 6.9 Hz, 3H). ^{13}C NMR (101 MHz, $CDCl_3$) δ 153.36, 147.85, 140.23, 138.81, 137.66, 131.34, 128.19, 122.35, 116.89, 113.75, 110.15, 42.16, 20.35. $[M + H]^+$ for $C_{13}H_{14}NOSe$ pred. 280.0235, meas. 280.0236; HPLC purity: 97.69%.

*5-((2-Methylallyl)selanyl)quinolin-8-ol (**8f**).* Yellow solid, yield 61%. Mp 59.7−60.3 °C. R_f = 0.22 (CH_2Cl_2/CH_3OH=20/1). ^{1}H NMR (400 MHz, $CDCl_3$) δ 8.84−8.67 (m, 2H), 7.81 (d, J = 7.9 Hz, 1H), 7.51 (dd, J = 8.4, 4.3 Hz, 1H), 7.09 (d, J = 7.9 Hz, 1H), 4.60−4.48 (m, 1H), 4.32 (d, J = 0.8 Hz, 1H), 3.46−3.30 (m, 2H), 1.85 (d, J = 0.4 Hz, 3H). ^{13}C NMR (101 MHz, $CDCl_3$) δ 158.97, 153.05, 146.33, 144.11, 142.05, 141.52, 135.68, 127.28, 121.51, 118.30, 116.04, 41.73, 25.97. $[M + H]^+$ for $C_{13}H_{14}NOSe$ pred. 280.0235, meas. 280.0234; HPLC purity: 98.72%.

*5-((3-Methylbut-2-en-1-yl)selanyl)quinolin-8-ol (**8g**).* Yellow solid, yield 66%. Mp 49.6−50.4 °C. R_f = 0.27 (CH_2Cl_2/CH_3OH = 20/1). ^{1}H NMR (400 MHz, $CDCl_3$) δ 8.78 (ddd, J = 6.4, 5.8, 1.5 Hz, 2H), 7.84 (d, J = 7.9 Hz, 1H), 7.51 (dd, J = 8.5, 4.2 Hz, 1H), 7.09 (d, J = 7.9 Hz, 1H), 5.28 (tdt, J = 8.4, 2.7, 1.3 Hz, 1H), 3.40 (d, J = 8.4 Hz, 2H), 1.52 (s, 3H), 1.10 (s, 3H). ^{13}C NMR (101 MHz, $CDCl_3$) δ 153.20, 147.80, 138.69, 137.94, 137.49, 135.60, 131.11, 122.14, 120.54, 117.16, 109.97, 27.40, 25.47, 16.97. $[M + H]^+$ for $C_{14}H_{16}NOSe$ pred. 294.0392, meas. 294.0393; HPLC purity: 95.89%.

*5-(But-3-en-1-ylselanyl)quinolin-8-ol (**8h**).* Yellow solid, yield 59%. Mp 37.7−38.9 °C. R_f = 0.29 (CH_2Cl_2/CH_3OH = 20/1). ^{1}H NMR (400 MHz, $CDCl_3$) δ 8.81−8.74 (m, 2H), 7.87 (d, J = 7.9 Hz, 1H), 7.53 (dd, J = 8.5, 4.2 Hz, 1H), 7.11 (d, J = 7.9 Hz, 1H), 5.83−5.72 (m, 1H), 5.04−5.01 (m, 1H), 4.99 (t, J = 1.3 Hz, 1H), 2.83 (t, J = 7.5 Hz, 2H), 2.34 (tt, J = 8.6, 1.2 Hz, 2H). ^{13}C NMR (101 MHz, $CDCl_3$) δ 152.09, 146.88, 137.85, 136.14, 136.04, 136.01, 129.67, 121.35, 115.73, 114.88, 109.25, 33.31, 27.26. $[M + H]^+$ for $C_{13}H_{14}NOSe$ pred. 280.0235, meas. 280.0235; HPLC purity: 97.43%.

*5-((2-(Piperidin-1-yl)ethyl)selanyl)quinolin-8-ol (**8i**).* Yellow solid, yield 56%. Mp 92.1−93.0 °C R_f = 0.19 (CH_2Cl_2/CH_3OH = 10/1). ^{1}H NMR (400 MHz, $CDCl_3$) δ 9.25 (d, J = 8.1 Hz, 1H), 9.07 (d, J = 4.3 Hz, 1H), 8.05 (d, J = 7.2 Hz, 1H), 7.85 (d, J = 6.2 Hz, 1H), 7.74 (d, J = 5.7 Hz, 1H), 3.72 (dd, J = 14.0, 7.0 Hz, 2H), 2.98 (dd, J = 10.8, 5.9 Hz, 2H), 2.10−1.90 (m, 4H), 1.26−1.21 (m, 6H). ^{13}C NMR (101 MHz, MeOD) δ 148.75, 144.78, 144.74, 141.71, 140.58, 124.40, 124.02, 117.38, 117.33, 58.18, 54.02, 32.48, 24.21, 22.64. $[M + H]^+$ for $C_{16}H_{21}N_2OSe$ pred. 337.0814, meas. 337.0816; HPLC purity: 98.32%.

Biological Assays. *ThT Assay.*[60,61] Aβ_{1-42} (Millipore, counterion: NaOH) was dissolved in ammonium hydroxide (1% v/v) to give a stock solution (2000 μM), which was aliquoted into small samples and stored at −80 °C.

For the inhibition of copper-mediated Aβ_{1-42} aggregation experiment, the Aβ stock solution was diluted in 20 μM HEPES (pH 6.6) with 150 μM NaCl. The mixture of the peptide (10 μL, 25 μM, final concentration) with or without copper (10 μL, 25 μM, final concentration) and the tested compound (10 μL, 50 μM, final concentration) was incubated at 37 °C for 24 h. Then 20 μL of the sample was diluted to a final volume of 200 μL with 50 mM glycine−NaOH buffer (pH 8.0) containing thioflavin T (5 μM). The detection method was the same as that of self-mediated Aβ_{1-42} aggregation experiment.

For the disaggregation of copper-induced Aβ fibrils experiment, the Aβ stock solution was diluted in 20 μM HEPES (pH 6.6) with 150 μM NaCl. The mixture of the peptide (10 μL, 25 μM, final concentration) with copper (10 μL, 25 μM, final concentration) was incubated at 37 °C for 24 h. The tested compound (10 μL, 50 μM, final concentration) was then added and incubated at 37 °C for another 24 h. Then 20 μL of the sample was diluted to a final volume of 200 μL with 50 mM glycine−NaOH buffer (pH 8.0) containing thioflavin T (5 μM). The detection method was the same as above.

TEM Assay.[34] For the copper-induced experiment, Aβ stock solution was diluted with 20 μM HEPES (pH = 6.6) and 150 μM NaCl. The sample preparation was same as that for the ThT assay.

Aliquots (10 μL) of the samples were placed on a carbon-coated copper/rhodium grid for 2 min. Each grid was stained with uranyl acetate (1%, 5 μL) for 2 min. After draining off the excess staining solution, the specimen was transferred for imaging in a transmission electron microscope (JEOL JEM-1400). All compounds were solubilized in the buffer which was used for the experiment.

Oxygen Radical Absorbance Capacity (ORAC-FL) Assay.[62,63] The tested compound and fluorescein (FL) stock solution were diluted with 75 mM phosphate buffer (pH 7.4) to 10 μM (or 20 μM) and 0.117 μM, respectively. The solution of (±)-6-hydroxy-2,5,7,8-tetramethylchroman-2-carboxylic acid (Trolox) was diluted with the same buffer to 100, 80, 60, 50, 40, 20, and 10 μM. The solution of 2,2′-azobis(amidinopropane)dihydrochloride (AAPH) was prepared before the experiment by dissolving 108.4 mg of AAPH in 10 mL of 75 mM phosphate buffer (pH 7.4) to a final concentration of 40 mM. The mixture of the tested compound (20 μL) and FL (120 μL; 70 nM, final concentration) was preincubated for 10 min at 37 °C, and then 60 μL of the AAPH solution was added. The fluorescence was recorded every minute for 120 min (excitation, 485 nm; emission, 520 nm). A blank using phosphate buffer instead of the tested compound was also carried out. All reaction mixtures were prepared in triplicate, and at least three independent runs were performed for each sample. The antioxidant curves (fluorescence versus time) were normalized to the curve of the blank. The area under the fluorescence decay curve (AUC) was calculated as following equation:

$$\mathrm{AUC} = 1 + \sum_{i=120}^{i=1} (f_i/f_0)$$

where f_0 is the initial fluorescence reading at 0 min and f_i is the fluorescence reading at time i. The net AUC was calculated by the expression: $\mathrm{AUC_{sample}} - \mathrm{AUC_{blank}}$. Regression equations between net AUC and Trolox concentrations were calculated. ORAC-FL values for each sample were calculated by using the standard curve which means the ORAC-FL value of tested compound expressed as Trolox equivalents.

Horseradish Peroxidase Assay.[44] The hydrogen peroxide scavenging property was measured using the horseradish peroxidase assay. Test compounds of 200 μL of different concentrations were incubated with 100 μL of 1 mM H_2O_2. Then, 0.1 M phosphate buffer (pH 7.4, 100 μL) and 0.1 M NaCl (50 μL) were added. The solution was incubated for 10 h at 37 °C. Then, a solution containing red phenol (0.2 mg/mL) and horseradish peroxidase (0.5 mg/mL) in 0.1 M phosphate buffer (500 μL) was added. After 15 min, 1 M NaOH solution (50 μL) was added to quench the reaction, and the absorbance was recorded at 610 nm. The result is expressed as the

dx.doi.org/10.1021/cn500119g | ACS Chem. Neurosci. 2014, 5, 952−962

percentage of reduction of H_2O_2. The percentage of H_2O_2 scavenging activity was calculated according to the following formula: $1 - (A_{sample} - A_{blank})/(A_{control} - A_{blank}) \times 100$, where A_{sample} is the absorbance of the samples, A_{blank} is the absorbance of the blank, and $A_{control}$ is the absorbance of the control.

In Vitro Blood-Brain Barrier Permeation Assay. The blood-brain barrier penetration of compounds was evaluated using the parallel artificial membrane permeation assay (PAMPA) described by Di et al.[59,61,64] Commercial drugs were purchased from Sigma and Alfa Aesar. Porcine brain lipid (PBL) was obtained from Avanti Polar Lipids. The donor microplate (PVDF membrane, pore size 0.45 mm) and acceptor microplate were both from Millipore. The 96-well UV plate (COSTAR) was from Corning Incorporated. The acceptor 96-well microplate was filled with 300 μL of PBS/EtOH (7:3), and the filter membrane was impregnated with 4 μL of PBL in dodecane (20 mg/mL). Compounds were dissolved in DMSO at 5 mg/mL and diluted 50-fold in PBS/EtOH (7:3) to a final concentration of 100 μg/mL. Then, 200 μL of the solution was added to the donor wells. The acceptor filter plate was carefully placed on the donor plate to form a sandwich, which was left undisturbed for 10 h at 25 °C. After incubation, the donor plate was carefully removed, and the concentration of compounds in the acceptor wells was determined using the UV plate reader (Flexstation 3). Every sample was analyzed at five wavelengths in four wells and in at least three independent runs. P_e was calculated by the following expression: $P_e = -V_dV_a/[(V_d + V_a)At] \ln(1 - \text{drug}_{acceptor}/\text{drug}_{equilibrium})$, where V_d is the volume of the donor well, V_a is the volume in the acceptor well, A is the filter area, t is the permeation time, $\text{drug}_{acceptor}$ is the the absorbance obtained in the acceptor well, and $\text{drug}_{equilibrium}$ is the the theoretical equilibrium absorbance. The results are given as the mean ± standard deviation. In the experiment, 13 quality control standards of known BBB permeability were included to validate the analysis set. A plot of the experimental data versus literature values gave a strong linear correlation, P_e (exp.) = 1.4574P_e (lit.) − 1.0773 (R^2 = 0.9427) (Supporting Information Figure S1). From this equation and the limit established by Di et al. (P_e (lit.) = 4.0 × 10^{-6} cm/s) for blood-brain barrier permeation, we concluded that compounds with a permeability greater than 4.7 × 10^{-6} cm/s could cross the blood-brain barrier (Supporting Information Table S2).

Metal-Chelating Study. The chelating studies were performed with a UV−vis spectrophotometer. All compounds were solubilized in the buffer which was used for the experiment. The absorption spectra of compound (50 μM, final concentration) alone or in the presence of $CuSO_4$, $FeSO_4$, or $ZnCl_2$ (50 μM, final concentration) for 30 min in buffer (20 mM HEPES, 150 mM NaCl, pH 7.4) were recorded at room temperature.

For the stoichiometry of the compound-Cu^{2+} complex, a fixed amount of **8a** (80 μM) was mixed with growing amounts of copper ion (0−144 μM), and the difference UV−vis spectra were examined to investigate the ratio of ligand/metal in the complex.

Determination of Cytotoxicity. The cytotoxicity was evaluated with the colorimetric MTT [3-(4,5-dimethyl-2-thiazolyl)-2,5-diphenyl-2H-tetrazolium bromide] assay. Human neuron-like cells, SH-SY5Y, were routinely grown at 37 °C in a humidified incubator with 5% CO_2 in Dulbecco's modified Eagle's medium (DMEM, GIBCO) supplemented with 10% fetal calf serum (FCS, GIBCO), 1 mM glutamine, 50 mg/μL penicillin, and 50 mg/μL streptomycin. SH-SY5Y cells were seeded at 5 × 10^4 cells/well in 96-well plates. After 24 h, the medium was removed and replaced with the tested compounds at different concentrations for 24 h at 37 °C. Then, the cells were incubated with MTT (2.5 mg/mL) in PBS for 4 h. After the removal of MTT, the formazan crystals were dissolved in DMSO. The amount of formazan was measured (570 nm). Cell viability was expressed as percentage of control cells and calculated by the formula $F_t/F_{nt} \times 100$, where F_t is the absorbance of treated neurones and F_{nt} is the absorbance of untreated neurones.

Antioxidant Activity in SH-SY5Y Cells. SH-SY5Y cells were seeded at 1 × 10^4 cells/well in 96-well plates; After 24 h, the medium was removed and replaced with tested compounds at 37 °C and kept for another 24 h. The cells were washed with PBS and incubated with 5 μM DCFH-DA (a fluorescent probe) in PBS at 37 °C in 5% CO_2 for 30 min. After removal of DCFH-DA and further washing, the cells were exposed to 0.1 mM *t*-BuOOH (a compound used to induce oxidative stress) in PBS for 30 min. At the end of the incubation, the fluorescence of the cells from each well was measured ($\lambda_{excitation}$ = 485 nm, $\lambda_{emission}$ = 535 nm) with a multifunctional microplate reader (Molecular Devices, Flex Station 3). The antioxidant activity was expressed as percentage of control cells and calculated by the formula $(F_t - F_{nt})/(F_t' - F_{nt}) \times 100$, where F_t is the absorbance of treated neurons with tested compound, F_t' is the absorbance of treated neurons without tested compound, and F_{nt} is the absorbance of neurons not treated with *t*-BuOOH.

Ascorbate Studies.[65] All of the solutions, except $CuSO_4$ (Milli-Q water only) and **8a** (dissolved in methanol and diluted in PBS), were mixed and diluted in a phosphate (20 mM), NaCl (100 mM) buffer (PBS) at pH 7.4 with a final sample volume of 200 μL. Each experiment was performed in triplicate. Hydroxyl radical production was measured as the conversion of CCA into 7-hydroxy-CCA ($\lambda_{excitation}$ = 395 nm, $\lambda_{emission}$ = 450 nm). The general order of addition was as follows: CCA [50 μM], ligand [15 μM], or copper [5 μM] and then ascorbate [150 μM]. All of the test solutions contained 1 μM desferryl and 0.1% methanol.

Statistical Analysis. The results are expressed as the mean ± SD of at least three independent experiments. Data were subjected to Student's *t* test or one-way analysis of variance (ANOVA) followed by Dunnett's test. *P* values less than 0.05 were accepted to indicate the significance.

■ ASSOCIATED CONTENT

Supporting Information

Tables with results of in vitro blood-brain barrier permeation assay; figure showing linear correlation between experiment and reported permeability of commercial drugs using the PAMPA-BBB assay. This material is available free of charge via the Internet at http://pubs.acs.org.

■ AUTHOR INFORMATION

Corresponding Authors

*Tel: +086-20-3994-3051. Fax: +086-20-3994-3051. E-mail: huangl72@mail.sysu.edu.cn.

*Tel: +086-20-3994-3050. Fax: +086-20-3994-3050. E-mail: lixsh@mail.sysu.edu.cn.

Author Contributions

Z.W., L.H., and X.L. take charge of the research. Z.W., Y.W., and W.L. synthesized compounds. Z.W. and Y.W. carried out antioxidation and meta bonding related assay. Z.W. and F.M. performed cell culture. Z.W., Y.W., and Y.S. determined BBB permeation. Z.W., L.H., and X.L. written the manuscript. All authors have given approval to the final version of the manuscript.

Funding

We thank the Natural Science Foundation of China (No. 21302235, 20972198) and the Ph.D. Programs Foundation of the Ministry of Education of China (20120171120045) for financial support of this study.

Notes

The authors declare no competing financial interest.

■ ABBREVIATIONS

AD, Alzheimer's disease; BBB, blood-brain barrier; DFO, desferrioxamine; EDTA, ethylenediaminetetraacetate; CQ, clioquinol; AChE, acetylcholinesterase; GPx, glutathione peroxidase; ORAC-FL, oxygen radical absorbance capacity with fluorescein; HRPA, horseradish peroxidase assay; CCA, coumarin-3-carboxylic acid; DCFH-DA, dichlorofluorescein

diacetate; MTT, 3-(4,5-dimethyl-2-thiazolyl)-2,5-diphenyl-2*H*-tetrazolium bromide; TEM, transmission electron microscopy; CNS, central nervous system; Aβ, β-amyloid; ROS, reactive oxygen species; PAMPA-BBB, parallel artificial membrane permeation assay for the blood-brain barrier; ThT, thioflavin T; TLC, thin-layer chromatography; PBL, porcine brain lipid

REFERENCES

(1) Walsh, D. M., and Selkoe, D. J. (2004) Deciphering the Molecular Basis of Memory Failure in Alzheimer's Disease. *Neuron 44*, 181−193.

(2) Scarpini, E., Schelterns, P., and Feldman, H. (2003) Treatment of Alzheimer's disease: Current status and new perspectives. *Lancet Neurol. 2*, 539−547.

(3) Dong, J., Atwood, C. S., Anderson, V. E., Siedlak, S. L., Smith, M. A., Perry, G., and Carey, P. R. (2003) Metal Binding and Oxidation of Amyloid-β within Isolated Senile Plaque Cores: Raman Microscopic Evidence. *Biochemistry 42*, 2768−2773.

(4) Bush, A. I. (2008) Drug Development Based on the Metals Hypothesis of Alzheimer's Disease. *J. Alzheimer's Dis. 15*, 223−240.

(5) Zecca, L., Youdim, H. B. M., Riederer, P., Connor, J. R., and Crichton, R. R. (2004) Iron, brain ageing and neurodegenerative disorders. *Nat. Rev. Neurosci. 5*, 863−873.

(6) Mandel, S., Amit, T., Bar-Am, O., and Youdim, M. B. H. (2007) Iron dysregulation in Alzheimer's disease: Multimodal brain permeable iron chelating drugs, possessing neuroprotective-neurorescue and amyloid precursor protein-processing regulatory activities as therapeutic agents. *Prog. Neurobiol. 82*, 348−360.

(7) Amit, T., Avramovich-Tirosh, Y., Youdim, M. B. H., and Mandel, S. (2008) Targeting multiple Alzheimer's disease etiologies with multimodal neuroprotective and neurorestorative iron chelators. *FASEB J. 22*, 1296−1305.

(8) Fernandez-Bachiller, M. I., Perez, C., Gonzalez-Munoz, G. C., Conde, S., Lopez, M. G., Villarroya, M., Garcia, A. G., and Rodriguez-Franco, M. I. (2010) Novel tacrine-8-hydroxyquinoline hybrids as multifunctional agents for the treatment of Alzheimer's disease, with neuroprotective, cholinergic, antioxidant, and copper-complexing properties. *J. Med. Chem. 53*, 4927−4937.

(9) Bonda, D. J., Wang, X., Perry, G., Nunomura, A., Tabaton, M., Zhu, X., and Smith, M. A. (2010) Oxidative stress in Alzheimer disease: A possibility for prevention. *Neuropharmacology 59*, 290−294.

(10) Von Bernhardi, R., and Eugenin, J. (2012) Alzheimer's disease: redox dysregulation as a common denominator for diverse pathogenic mechanisms. *Antioxid. Redox Signaling 16*, 974−1031.

(11) Rayman, M. P. (2000) The importance of selenium to human health. *Lancet 356*, 233−241.

(12) Jacob, C., Giles, G. I., Giles, N. M., and Sies, H. (2003) Sulfur and Selenium: The Role of Oxidation State in Protein Structure and Function. *Angew. Chem., Int. Ed. Engl. 42*, 4742−4758.

(13) Kryukov, G. V., Castellano, S., Novoselov, S. V., Lobanov, A. V., Zehtab, O., Guigó, R., and Gladyshev, V. N. (2003) Characterization of Mammalian Selenoproteomes. *Science 300*, 1439−1443.

(14) Nascimento, V., Alberto, E. E., Tondo, D. W., Dambrowski, D., Detty, M. R., Nome, F., and Braga, A. L. (2012) GPx-Like activity of selenides and selenoxides: experimental evidence for the involvement of hydroxy perhydroxy selenane as the active species. *J. Am. Chem. Soc. 134*, 138−141.

(15) Trippier, P. C., Jansen Labby, K., Hawker, D. D., Mataka, J. J., and Silverman, R. B. (2013) Target- and mechanism-based therapeutics for neurodegenerative diseases: strength in numbers. *J. Med. Chem. 56*, 3121−3147.

(16) Tapiero, H., Townsend, D. M., and Tew, K. D. (2003) The antioxidant role of selenium and seleno-compounds. *Biomed. Pharmacother. 57*, 134−144.

(17) Magalhães, J. P. d., and Church, G. M. (2006) Cells discover fire: Employing reactive oxygen species in developmentand consequences for aging. *Exp. Gerontol. 41*, 1−10.

(18) Nordberg, J., and Arnér, E. S. J. (2001) Reactive oxygen species, antioxidants, and the mammalian thioredoxin system. *Free Radical Biol. Med. 31*, 1287−1312.

(19) Mugesh, G., du Mont, W.-W., and Sies, H. (2001) Chemistry of Biologically Important Synthetic Organoselenium Compounds. *Chem. Rev. 101*, 2125−2180.

(20) Sarma, B. K., Manna, D., Minoura, M., and Mugesh, G. (2010) Synthesis, Structure, Spirocyclization Mechanism, and Glutathione Peroxidase-like Antioxidant Activity of Stable Spirodiazaselenurane and Spirodiazatellurane. *J. Am. Chem. Soc. 132*, 5364−5374.

(21) Sarma, B. K., and Mugesh, G. (2005) Glutathione Peroxidase (GPx)-like Antioxidant Activity of the Organoselenium Drug Ebselen: Unexpected Complications with Thiol Exchange Reactions. *J. Am. Chem. Soc. 127*, 11477−11485.

(22) Zhao, R., Masayasu, H., and Holmgren, A. (2002) Ebselen: A substrate for human thioredoxin reductase strongly stimulating its hydroperoxide reductase activity and a superfast thioredoxin oxidant. *Proc. Natl. Acad. Sci. U.S.A. 99*, 8579−8584.

(23) Nogueira, C. W., Zeni, G., and Rocha, J. B. T. (2004) Organoselenium and Organotellurium Compounds: Toxicology and Pharmacology. *Chem. Rev. 104*, 6255−6286.

(24) Bar-Am, O., Amit, T., Weinreb, O., Youdim, M. B. H, and Mandel, S. (2010) Propargylamine containing compounds as modulators of proteolytic cleavage of amyloid-beta protein precursor: involvement of MAPK and PKC activation. *J. Alzheimer's Dis. 21*, 361−371.

(25) Weinreb, O., Amit, T., Bar-Am, O., and Youdim, M. B. H. (2010) Rasagiline: A novel anti-Parkinsonian monoamine oxidase-B inhibitor with neuroprotective activity. *Prog. Neurobiol. 92*, 330−344.

(26) Maruyama, W., Akao, Y., Carrillo, M. C., Kitani, K.-i., Youdium, M. B. H., and Naoi, M. (2002) Neuroprotection by propargylamines in Parkinson's disease: Suppression of apoptosis and induction of prosurvival genes. *Neurotoxicol. Teratol. 24*, 675−682.

(27) Rucins, M., Kaldre, D., Pajuste, K., Fernandes, M. A. S., Vicente, J. A. F., Klimaviciusa, L., Jaschenko, E., Kanepe-Lapsa, I., Shestakova, I., Plotniece, M., Gosteva, M., Sobolev, A., Jansone, B., Muceniece, R., Klusa, V., and Plotniece, A. (2014) Synthesis and studies of calcium channel blocking and antioxidant activities of novel 4-pyridinium and/or N-propargyl substituted 1,4-dihydropyridine derivatives. *C. R. Chim. 17*, 69−80.

(28) Youdim, M. B. H., Bar Am, O., Yogev-Falach, M., Weinreb, O., Maruyama, W., Naoi, M., and Amit, T. (2005) Rasagiline: Neurodegeneration, neuroprotection, and mitochondrial permeability transition. *J. Neurosci. Res. 79*, 172−179.

(29) Zheng, H., Weiner, L. M., Bar-Am, O., Epsztejn, S., Cabantchik, Z. I., Warshawsky, A., Youdim, M. B. H., and Fridkin, M. (2005) Design, synthesis, and evaluation of novel bifunctional iron-chelators as potential agents for neuroprotection in Alzheimer's, Parkinson's, and other neurodegenerative diseases. *Bioorg. Med. Chem. 13*, 773−783.

(30) Dragoni, S., Porcari, V., Valoti, M., Travagli, M., and Castagnolo, D. (2006) Antioxidant properties of propargylamine derivatives: assessment of their ability to scavenge peroxynitrite. *J. Pharm. Pharmacol. 58*, 561−565.

(31) Bar-Am, Orit, Weinreb, Orly, Amit, Tamar, and Youdim, M. B. H. (2005) Regulation of Bcl-2 family proteins, neurotrophic factors, and APP processing in the neurorescue activity of propargylamine. *FASEB J. 19*, 1899−1901.

(32) Yu, P. H., Davis, B. A., and Boulton, A. A. (1992) Aliphatic Propargylamines: Potent, Selective, Irreversible Monoamine Oxidase B Inhibitors. *J. Med. Chem. 35*, 3705−3713.

(33) Avramovich-Tirosh, Y., Amit, T., Bar-Am, O., Zheng, H., Fridkin, M., and Youdim, M. B. H. (2007) Therapeutic targets and potential of the novel brain- permeable multifunctional iron chelator−monoamine oxidase inhibitor drug, M-30, for the treatment of Alzheimer's disease. *J. Neurochem. 100*, 490−502.

(34) Gal, S., Zheng, H., Fridkin, M., and Youdim, M. B. H. (2005) Novel multifunctional neuroprotective iron chelator-monoamine oxidase inhibitor drugs for neurodegenerative diseases. In vivo

selective brain monoamine oxidase inhibition and prevention of MPTP-induced striatal dopamine depletion. *J. Neurochem. 95*, 79−88.
(35) Luo, Z., Sheng, J., Sun, Y., Lu, C., Yan, J., Liu, A., Luo, H.-b., Huang, L., and Li, X. (2013) Synthesis and Evaluation of Multi-Target-Directed Ligands against Alzheimer's Disease Based on the Fusion of Donepezil and Ebselen. *J. Med. Chem. 56*, 9089−9099.
(36) Luo, Z., Liang, L., Sheng, J., Pang, Y., Li, J., Huang, L., and Li, X. (2014) Synthesis and biological evaluation of a new series of ebselen derivatives as glutathione peroxidase (GPx) mimics and cholinesterase inhibitors against Alzheimer's disease. *Bioorg. Med. Chem. 22*, 1355−1361.
(37) Patel, N. B., Patel, J. C., and Modi, S. H. (2011) Synthesis and antimicrobial activity of carbonyl pyridoquinolones containing urea and piperazine residue. *J. Saudi Chem. Soc. 15*, 167−176.
(38) Mazumder, U. K., Gupta, M., Bhattacharya, S., Karki, S. S., Rathinasamy, S., and Thangavel, S. (2004) Antineoplastic and antibacterial activity of some mononuclear Ru(II) complexes. *J. Enzyme Inhib. Med. Chem. 19*, 185−92.
(39) Liu, J. O.; Shim, J., Sup.; Chong, C. R.; Bhat, S. Preparation of quinoline derivatives for use as human methionine aminopeptidase, sirT1 and angiogenesis inhibitors. Patent: WO 2010/042163 A2, 2010.
(40) Ou, B., Hampsch-Woodill, M., and Prior, R. L. (2001) Development and Validation of an Improved Oxygen Radical Absorbance Capacity Assay Using Fluorescein as the Fluorescent Probe. *J. Agric. Food. Chem. 49*, 4619−4626.
(41) Dávalos, A., Gómez-Cordovés, C., and Bartolomé, B. (2004) Extending Applicability of the Oxygen Radical Absorbance Capacity (ORAC−Fluorescein) Assay. *J. Agric. Food. Chem. 52*, 48−54.
(42) Ning, X., Guo, Y., Wang, X., Ma, X., Tian, C., Shi, X., Zhu, R., Cheng, C., Du, Y., Ma, Z., Zhang, Z., and Liu, J. (2014) Design, synthesis, and biological evaluation of (e)-3,4-dihydroxystyryl aralkyl sulfones and sulfoxides as novel multifunctional neuroprotective agents. *J. Med. Chem. 57*, 4302−4312.
(43) Sultana, R., Newman, S., Mohmmad-Abdul, H., Keller, J. N., and Butterfield, D. A. (2004) Protective Effect of the Xanthate, D609, on Alzheimer's Amyloid β-peptide (1−42)-Induced Oxidative Stress in Primary Neuronal Cells. *Free Radical Res. 38*, 449−558.
(44) Merino-Montiel, P., López, Ó., and Fernández-Bolaños, J. G. (2012) l-Isofucoselenofagomine and derivatives: Dual activities as antioxidants and as glycosidase inhibitors. *Tetrahedron 68*, 3591−3595.
(45) Riederer, P., Danielczyk, W., and Grünblatt, E. (2004) Monoamine Oxidase-B Inhibition in Alzheimer's Disease. *Neurotoxicology 25*, 271−277.
(46) Oyama, Y., Hayashi, A., Ueha, T., and Maekawa, K. (1994) Characterization of 2′,7′-dichlorofluorescin fluorescence in dissociated mammalian brain neurons: estimation on intracellular content of hydrogen peroxide. *Brain Res. 635*, 113−117.
(47) Sharma, A. K., Pavlova, S. T., Kim, J., Finkelstein, D., Hawco, N. J., Rath, N. P., Kim, J., and Mirica, L. M. (2012) Bifunctional Compounds for Controlling Metal-Mediated Aggregation of the Aβ42 Peptide. *J. Am. Chem. Soc. 134*, 6625−6636.
(48) Lee, S., Zheng, X., Krishnamoorthy, J., Savelieff, M. G., Park, H. M., Brender, J. R., Kim, J. H., Derrick, J. S., Kochi, A., Lee, H. J., Kim, C., Ramamoorthy, A., Bowers, M. T., and Lim, M. H. (2014) Rational design of a structural framework with potential use to develop chemical reagents that target and modulate multiple facets of Alzheimer's disease. *J. Am. Chem. Soc. 136*, 299−310.
(49) Baum, L., and Ng, A. (2004) Curcumin interaction with copper and iron suggests one possible mechanism of action in Alzheimer's disease animal models. *J. Alzheimer's Dis. 6*, 367−377.
(50) Bolognesi, M. L., Cavalli, A., Valgimigli, L., Bartolini, M., Rosini, M., Andrisano, V., Recanatini, M., and Melchiorre, C. (2007) Multi-Target-Directed Drug Design Strategy: From a Dual Binding Site Acetylcholinesterase Inhibitor to a Trifunctional Compound against Alzheimer's Disease. *J. Med. Chem. 50*, 6446−6449.
(51) Geng, J., Li, M., Wu, L., Ren, J., and Qu, X. (2012) Liberation of Copper from Amyloid Plaques: Making a Risk Factor Useful for Alzheimer's Disease Treatment. *J. Med. Chem. 55*, 9146−9155.
(52) Xu, L., Xu, Y., Zhu, W., Yang, C., Han, L., and Qian, X. (2012) A highly selective and sensitive fluorescence "turn-on" probe for Ag^+ in aqueous solution and live cells. *Dalton Trans. 41*, 7212−7217.
(53) Saharan, S., and Mandal, P. K. (2014) The emerging role of glutathione in Alzheimer's disease. *J. Alzheimer's Dis. 40*, 519−529.
(54) Bush, A. I. (2003) The metallobiology of Alzheimer's disease. *Trends Neurosci. 26*, 207−214.
(55) Gaggelli, E., Kozlowski, H., Valensin, D., and Valensin, G. (2006) Copper Homeostasis and Neurodegenerative Disorders (Alzheimer's, Prion, and Parkinson's Diseases and Amyotrophic Lateral Sclerosis). *Chem. Rev. 106*, 1995−2044.
(56) Barnham, K. J., and Masters, C. L. (2004) Neurodegenerative diseases and oxidative stress. *Nat. Rev. Drug Discovery 3*, 205−214.
(57) Hardeland, R. (2005) Atioxidative protection by melatonin. *Endocrine 27*, 119−130.
(58) Lynch, M. A. (2004) Long-Term Potentiation and Memory. *Physiol. Rev. 84*, 87−136.
(59) Di, L., Kerns, E. H., Fan, K., McConnell, O. J., and Carter, G. T. (2003) High throughput artificial membrane permeability assay for blood−brain barrier. *Eur. J. Med. Chem. 38*, 223−232.
(60) Rosini, M., Simoni, E., Bartolini, M., Cavalli, A., Ceccarini, L., Pascu, N., McClymont, D. W., Tarozzi, A., Bolognesi, M. L., Minarini, A., Tumiatti, V., Andrisano, V., Mellor, I. R., and Melchiorre, C. (2008) Inhibition of Acetylcholinesterase, β-Amyloid Aggregation, and NMDA Receptors in Alzheimer's Disease: A Promising Direction for the Multi-target-Directed Ligands Gold Rush. *J. Med. Chem. 51*, 4381−4384.
(61) Camps, P., Formosa, X., Galdeano, C., Muñoz-Torrero, D., Ramírez, L., Gómez, E., Isambert, N., Lavilla, R., Badia, A., Clos, M. V., Bartolini, M., Mancini, F., Andrisano, V., Arce, M. P., Rodríguez-Franco, M. I., Huertas, Ó., Dafni, T., and Luque, F. J. (2009) Pyrano[3,2-c]quinoline−6-Chlorotacrine Hybrids as a Novel Family of Acetylcholinesterase- and β-Amyloid-Directed Anti-Alzheimer Compounds. *J. Med. Chem. 52*, 5365−5379.
(62) Choi, J.-S., Braymer, J. J., Nanga, R. P. R., Ramamoorthy, A., and Lim, M. H. (2010) Design of small molecules that target metal-Aβ species and regulate metal-induced Aβ aggregation and neurotoxicity. *Proc. Natl. Acad. Sci. U.S.A. 107*, 21990−21995.
(63) Rodríguez-Franco, M. I., Fernández-Bachiller, M. I., Pérez, C., Hernández-Ledesma, B., and Bartolomé, B. (2006) Novel Tacrine−Melatonin Hybrids as Dual-Acting Drugs for Alzheimer Disease, with Improved Acetylcholinesterase Inhibitory and Antioxidant Properties. *J. Med. Chem. 49*, 459−462.
(64) Wohnsland, F., and Faller, B. (2001) High-Throughput Permeability pH Profile and High-Throughput Alkane/Water log P with Artificial Membranes. *J. Med. Chem. 44*, 923−930.
(65) Guilloreau, L., Combalbert, S., Sournia-Saquet, A., Mazarguil, H., and Faller, P. (2007) Redox Chemistry of Copper−Amyloid-β: The Generation of Hydroxyl Radical in the Presence of Ascorbate is Linked to Redox-Potentials and Aggregation State. *ChemBioChem 8*, 1317−1325.